Interface Hamiltonian with a position-dependent stiffness: A nonlinear functional renormalization group study

C. J. Boulter
Laboratorium voor Vaste-Stoffysica en Magnetisme, Katholieke Universiteit Leuven, B-3001 Leuven, Belgium
(Received 26 September 1997)

A detailed study of the wetting behavior predicted from an effective interfacial Hamiltonian approach which allows for a position-dependent stiffness coefficient is given. A nonlinear functional renormalization group scheme is introduced enabling earlier studies to be extended into general dimensions $1<d\leqslant 3$ while permitting a semiquantitative numerical analysis. We find that the prediction of Fisher and Jin of a bare critical wetting transition being driven fluctuation-induced first order can occur for dimensions $d>d_c\approx 2.41$ while at lower d the transition remains critical. For $d>d_c$ first-order wetting is found if the wetting parameter $\omega(T)$ is less than a tricritical value $\omega_t(T)$. Importantly in three dimensions numerical analysis reveals $\omega_t>\omega$ thus clearly supporting the premise that the wetting transition in this case is indeed first order. We focus especially on demonstrating the robustness of this result under variation of the stiffness strength and renormalization group rescaling parameter. [S1063-651X(98)14002-3]

PACS number(s): 68.45.Gd, 64.60.Fr, 82.65.Dp, 68.10.−m

I. INTRODUCTION

The study of wetting transitions in systems with short-range interactions has attracted a great deal of interest over recent years [1–16]. One source of controversy has been an apparent discrepancy in three dimensions between theoretical predictions [5,6,10], primarily based on the renormalization group (RG), and Monte Carlo (MC) simulation results of critical [7] and complete wetting [14]. These discrepancies have now, to some extent, been accounted for by extending the model Hamiltonian to include fluctuations near the wall or surface which couple to the fluctuations in the unbinding interface. A detailed discussion can be found in [17,18]. However, the implication of these analyses is that current MC simulations of critical wetting do not probe the full asymptotic behavior. In other words, results of the present simulations, modeled in slab geometries, cannot be used for direct comparison with theoretical predictions relating to the unbinding of the interface in a semi-infinite system. Indeed a recent application of the Ginzburg criterion for the susceptibility χ_1 applied to models including these ''surface fluctuations'' reveals that crossover from mean-field behavior occurs only for values of the bulk magnetic field $h\lesssim 10^{-6}$ [18,19], several decades smaller than the values studied in the simulations [7]. Thus we should not expect to investigate the true asymptotic behavior using current simulation techniques because such regions in the field cannot be reached due to technical problems such as critical slowing down in the bulk and of interface fluctuations.

As a result we must presently rely on theoretical predictions for our understanding of wetting in a semi-infinite geometry. With this in mind we should start by asking perhaps the most fundamental question: ''What is the order of the transition in these systems?'' The answer to this basic question is far from clear and it is this issue that we address in the present paper. In particular, we wish to understand whether a transition which is critical at the bare mean-field level may become first order when fluctuations are included, as recently predicted by Fisher and Jin (FJ) [12,13]—and if so for which values of external parameters (dimension, temperature, etc.) does this occur? This analysis should be viewed as complementary to the ''two-field'' approach discussed above—in that work (see, for example, [17]) the surface fluctuations are shown to be crucial in understanding the MC simulations but do not affect the order of the transition and hence are not directly relevant for the issues we address here. In this paper we shall argue, on the basis of a nonlinear functional RG study, that in $d=3$ for temperatures above the roughening temperature the bare critical wetting transition *is* driven first order assuming currently accepted values for the bulk correlation length, etc. Conversely in $d=2$ the transition *always* remains critical so that the presence of a position-dependent stiffness coefficient plays no role, at least at the level of the order of the transition. At an intermediate dimension $d_c\approx 2.41$ there is a crossover between these two behaviors due to an additional fixed-point potential entering the analysis. A preliminary account of some of this work was given in [20], however, the details of the extended RG scheme are presented here along with a careful check on the robustness of our central conclusions.

The remainder of this paper is arranged as follows. In the next section the standard effective interface Hamiltonian and the improved Fisher-Jin model incorporating a position-dependent stiffness coefficient are introduced and RG predictions based on these models are discussed. In Sec. III we recall some details of the nonlinear functional RG and introduce a modified approximation scheme which allows for the presence of a position-dependent stiffness coefficient in the effective Hamiltonian. The numerical results obtained from this functional RG are described in Sec. IV both for a fixed rescaling parameter and in the infinitesimal rescaling limit. Finally in Sec. V a summary and discussion of the main results are provided.

II. EFFECTIVE HAMILTONIAN MODELS

We begin by recalling some pertinent details of the critical wetting transition and the effective Hamiltonian models

used to describe it. Consider a wall or substrate in the plane $z=0$ bounding a d-dimensional semi-infinite volume $(\mathbf{y},z>0)$. In this half space we imagine there is a medium at (or very close to) bulk coexistence between two phases, α and β say. We further assert that far away from the wall (i.e., $z\to\infty$) the α phase is stable while the wall exerts a preference for the β phase through the action of short-range interactions, such that a wetting layer of phase β exists close to the wall. An α-β interface separating this wetting layer from the bulk phase is located at a distance $l(\mathbf{y})$ from the wall. We assume that there exists a subcritical wetting temperature T_W such that as the temperature T is increased to T_W the mean thickness of the wetting layer diverges continuously—this interface delocalization transition is denoted critical wetting. Alternatively, if the wetting layer thickness diverges discontinuously we have a first-order wetting transition.

In this paper we restrict our attention to the case of short-range fluid-fluid forces (henceforth we consider α and β to be fluid phases) in addition to the short-range wall-fluid interaction discussed above. In this case the upper critical dimension is $d=3$ [4] so that to study wetting phenomena in $d\leqslant 3$ we generally have to go beyond mean-field (MF) theory using renormalization group techniques. These RG approaches are based on an effective interfacial Hamiltonian $H[l(\mathbf{y})]$ which is a functional of the wetting layer thickness. In particular, it has been typical to assume the simple interfacial or *capillary-wave* model [3]

$$H[l]=\int d^{d-1}y\{\tfrac{1}{2}\Sigma_0[\boldsymbol{\nabla} l(\mathbf{y})]^2+V(l(\mathbf{y}))\}, \qquad (2.1)$$

where $\Sigma_0=\Sigma_0(T,\ldots)$ is the interfacial tension or stiffness of a free α-β interface (and is thus independent of l) and $V(l)$ is the wall-interface binding potential which takes the form

$$V(l)=\overline{h}l+v_1e^{-\kappa l}+v_2e^{-2\kappa l}+\cdots . \qquad (2.2)$$

Here $\kappa\equiv 1/\xi_b$ is the inverse bulk correlation length of the wetting (β) phase and $\overline{h}$ is a measure of the (chemical potential) deviation from bulk two-phase coexistence.

A. Linear RG results

In $d=3$ linear RG analyses [3,5] of critical wetting ($\overline{h}=0$, $T\to T_W^-$) based on Eq. (2.1) have predicted remarkable nonuniversal behavior for both critical amplitudes and critical exponents with results depending sensitively on the dimensionless *wetting parameter* ω defined as

$$\omega(T;d=3)=\frac{k_BT}{4\pi\Sigma_0\xi_b^2}. \qquad (2.3)$$

Three regimes are predicted with, for example, the exponent $\nu_\parallel$, which measures the divergence of the transverse correlation length $\xi_\parallel$ along the edge of the wetting layer, being given by

$$\nu_\parallel=\begin{cases}(1-\omega)^{-1}, & 0\leqslant\omega<\frac{1}{2}\\ (\sqrt{2}-\sqrt{\omega})^{-2}, & \frac{1}{2}<\omega<2\\ \infty, & \omega>2\end{cases} \qquad (2.4)$$

where the final regime implies an exponentially fast divergence. Within the first two regimes ($\omega<2$) the fluctuations do not renormalize the wetting temperature so $T_W=T_W^{\mathrm{MF}}$ where T_W^{MF} is the mean-field wetting temperature. For $\omega>2$, T_W is predicted to be reduced below its MF value.

B. Nonlinear RG results

The predictions described above rest on a linearization of the exact functional RG. As a result these analyses are unable to consider a true hard wall but instead employ a soft or finite wall [such that the interface can actually fluctuate *behind* the wall: $l(\mathbf{y})<0$]. A comprehensive study by Lipowsky and Fisher (LF) [6] overcomes this problem and yields semiquantitative results in dimensions $d\leqslant 3$. Their analysis is based on a nonlinear functional RG (NFRG) scheme which is an approximate nonperturbative technique. Some of the technical details concerning the NFRG are given in Sec. III where a modified scheme is introduced. Here we briefly discuss the study of LF for the model (2.1) which consists of renormalizing the bare potential $V^{(0)}(l)$ via successive applications of a recursion relation $V^{(N+1)}(l)=\mathcal{R}[V^{(N)}(l)]$ [21]. Thus the critical behavior is governed by the fixed-point potentials, $V^*(l)$ say, which remain invariant under $\mathcal{R}$.

The most interesting phenomena occur for the specific scaling regime in which both exponents and phase boundaries are nontrivial. This so-called *strong-fluctuation regime* (SFL) is characterized by microscopic interactions satisfying

$$V(l)l^\tau\to 0 \quad \text{as} \quad l\to\infty, \qquad (2.5)$$

with

$$\tau\equiv\frac{2(d-1)}{(3-d)} \qquad (2.6)$$

$(1<d\leqslant 3)$. For $d<3$ a binding potential which decays faster than any power, as is the case for the systems with short-range interactions which we are focussing on, is always within the SFL. In this regime, for fixed $d<3$, LF found two nontrivial fixed-point potentials, namely, (i) a critical potential $V_c^*(l)$ with an attractive tail for large l, representing the bound interface and (ii) a purely repulsive potential $V_0^*(l)>0$ corresponding to the unbound interface. These potentials are shown schematically in Fig. 1. The surprising feature of these fixed points is that on the approach to $d=3$ they do not coalesce with the standard Gaussian fixed point as would be expected from analogy with typical bulk critical phenomena. Rather, for $d\to 3^-$ the two fixed-point potentials mutually annihilate leaving behind a line of ''drifting fixed points''—i.e., potentials whose *shape* is not affected by an application of the recursion operator $\mathcal{R}$ but whose *location* drifts steadily under successive iterations. By examining which fixed point an initial bare potential flows towards under $\mathcal{R}$, LF were able to locate numerically the wetting transition phase boundary for the range of dimensions $2\leqslant d\leqslant 3$. In $d=3$ the general features of the phase boundary agree with those determined from the linear RG analyses—i.e., the wetting temperature is unchanged for $\omega<2$ but is reduced below its MF value for $\omega>2$. The critical exponent $\nu_\parallel$ is determined via an eigen-

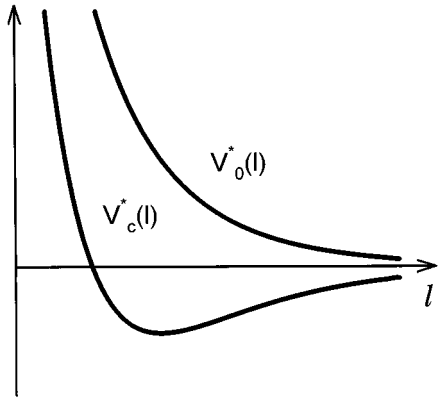

FIG. 1. Schematic representation of the two fixed-point binding potentials relevant for mapping out the phase diagram of the capillary-wave model. The purely repulsive potential $V_0^*(l)$ corresponds to the unbound interface while the critical potential $V_c^*(l)$ represents a bound interface.

perturbation analysis and in $d=2$ is found to be in remarkable agreement with the known exact result $\nu_\parallel=2$ [22]. Extrapolation to $d=3$ reveals that $\nu_\parallel$ diverges to the SFL result, $\nu_\parallel=\infty$ [regime 3 of Eq. (2.4)].

David and Leibler (DL) [11] have since shown that the picture of fixed-point potentials is even richer than first predicted. These authors found that on approaching $d=3$ numerous multicritical fixed points appear successively in pairs (V_m^*, W_m^*), $m=2,3,\ldots$ (retaining the notation of DL). The first pair $V_2^*(l)$ and $W_2^*(l)$ appear for $\tau\approx 4.8$ (corresponding to $d\approx 2.41$) and each has a maximum and two minima (including the one at $l=\infty$). In general $V_m^*(l)$ and $W_m^*(l)$ possess $m+1$ extrema including that at $l=\infty$. For $\tau\to\infty (d\to 3^-)$ V_0^*, V_c^*, and all the V_m^* $(m=2,3,\ldots)$ merge into the drifting fixed point discussed above. The W_m^* also attain the form of the drifting fixed point at large l while for small l the picture is less clear (see [11]). However, it should be stressed that these extra fixed points do not enter the phase boundary analysis of LF, hence their results are unaffected.

C. The Fisher-Jin model

The above analyses all take the standard capillary-wave Hamiltonian (2.1) as their starting point. This model has recently been questioned by Fisher and Jin, who have systematically derived an effective interfacial Hamiltonian starting from the more microscopic Landau-Ginzburg-Wilson (LGW) model

$$H_{\mathrm{LGW}}[m]=\int d\mathbf{y}\{[\tfrac{1}{2}(\boldsymbol{\nabla} m)^2+\phi(m)]dz+\phi_1(m(z=0))\}. \tag{2.7}$$

Here $m(r=(y,z))$ is the bulk order parameter and $\phi(m)$ is the bulk free-energy density which is a double-well function with two equal minima at two-phase coexistence. The surface potential ϕ_1 is modeled by the truncated expansion $\phi_1(m)=-h_1 m-g m^2/2$ where h_1 and g are the surface field and surface coupling enhancement, respectively. An interface Hamiltonian can be formally derived from Eq. (2.7) via the introduction of a constraint which specifies restrictions on the accessible microstates of H_{LGW} that are compatible with the given interfacial configuration $z=l(\mathbf{y})$. Thus $H[l]$ is defined through

$$\exp\{-H[l(\mathbf{y})]\}\equiv \mathrm{Tr}'(\exp\{-H_{\mathrm{LGW}}[m(\mathbf{r})]\}), \tag{2.8}$$

where the prime denotes that the trace is taken only over bulk states which satisfy the constraint.

In practice a saddle-point approximation for the trace in Eq. (2.8) is used. In this way FJ have shown that Eq. (2.1) should be replaced by the modified effective interface Hamiltonian

$$H[l]=\int d^{d-1}y\{\tfrac{1}{2}\Sigma(l)(\boldsymbol{\nabla} l)^2+V(l)\}. \tag{2.9}$$

The first difference between their model and the earlier one is that the coefficients v_n in the expansion for $V(l)$ [see Eq. (2.2)] are no longer l independent but are found to be polynomials in l of order n. Inclusion of these terms within the framework of the linear RG theory does not lead to any significant change in the predictions for critical wetting [23]. The second and more dramatic difference is the presence of a *position-dependent stiffness coefficient* replacing the free interface stiffness Σ_0. In particular, FJ observe $\Sigma(l)=\Sigma_0+\Delta\Sigma(l)$ where $\Delta\Sigma(l)\to 0$ as $l\to\infty$ and is given by an expansion similar to that of $V(l)$, namely,

$$\Delta\Sigma(l;T,\ldots)=(s_{10}+s_{11}\kappa l)e^{-\kappa l}+(s_{20}+s_{21}\kappa l+s_{22}(\kappa l)^2)e^{-2\kappa l}+\cdots . \tag{2.10}$$

At MF level close to critical wetting the dominant contribution is found to be $s_{21}\kappa l e^{-2\kappa l}$ where s_{21} takes a negative nonvanishing value.

The position-dependent stiffness cannot be incorporated into the existing NFRG so FJ restricted their analysis of Eq. (2.9) to an extended linear RG study in $d=3$. Although the analysis is more complicated due to a coupling between the RG flows of $\Delta\Sigma^{(t)}$ and $V^{(t)}$, where $e^t\geqslant 1$ is the spatial rescaling factor, their results can be written in a surprisingly simple form. In particular, they find that the binding potential $V^{(t)}(l)$ renormalizes exactly as in the $\Sigma(l)=\Sigma_0$ case except with the initial bare potential $V^{(0)}(l)$ being replaced by the effective potential

$$V_{\mathrm{eff}}(l)=V^{(0)}(l)+\frac{\omega\Lambda^2}{2\kappa^2}(1-e^{-2t})\Delta\Sigma^{(0)}(l), \tag{2.11}$$

where Λ is a nonuniversal momentum cutoff (see later). For large t this simply amounts to changing $V^{(0)}$ by a term proportional to $\Delta\Sigma^{(0)}$. For values of ω less than a tricritical value ω_t, FJ find that this leads to the negative dominant contribution to $\Delta\Sigma$ destabilizing the critical wetting transition and leading instead to a weakly first-order transition. For $\omega>\omega_t$ the transition remains critical. The value of ω_t was estimated to be in the region $0.5<\omega_t<1.0$ while a recent computation of $\omega(T)$ for the simple cubic Ising model predicts $\omega=0.78\pm 0.09$ for relevant temperatures [24]. Thus it is certainly possible that in $d=3$ the transition is fluctuation-induced first order although a more accurate determination of

ω_t is required prior to making firm predictions. The *stiffness instability mechanism* described above can occur only if there is some region in phase space where first-order wetting is possible so this mechanism cannot persist in the $d=2$ limit where it is known from exact results that the wetting transition is always critical [22]. In order to gain improved quantitative results in $d=3$ and better understand the picture for $2<d<3$ we now develop an extended NFRG suitable for studying Eq. (2.9).

III. THE NONLINEAR FUNCTIONAL RG

In this section we describe an extension of the approximate recursion relations developed by Wilson in the context of bulk critical phenomena [25] and LF for interfacial phenomena [6,26] which will allow us to investigate Eq. (2.9). Recall that the main disadvantage of the Wilson scheme as applied to bulk criticality is that it unavoidably forces the critical point decay exponent η to vanish [27] instead of attaining its proper (nonzero) value. In contrast the RG approach is particularly well suited to the study of unbinding phenomena because in this case the exponent η is identically equal to zero [6]. Thus we have considerable confidence in the reliability of the NFRG scheme when applied to wetting phenomena.

A. Formalism and approximations

Implicit in the definition of the effective interface models (2.1) and (2.9) is a momentum cutoff Λ (or equivalently a short-distance cutoff Λ^{-1}) so that in Fourier space the components of $l(\mathbf{y})$ only have wave numbers satisfying $|\mathbf{k}|<\Lambda$. In order to justify ignoring possible overhangs, bubbles, and higher-order terms the cutoff is required to satisfy $\Lambda^{d-1} \ll (\Sigma_0/k_BT)$, corresponding to length scales much greater than the bulk correlation length [1]. The renormalization group procedure consists of performing a partial trace in the partition function over small scale fluctuations, $l^{>}(\mathbf{y})$ say, with wave numbers in the range $\Lambda/b<|\mathbf{k}|<\Lambda$ where $b>1$ is an arbitrary rescaling factor. The partial trace over $l^{>}(\mathbf{y})$ yields a new, intermediate Hamiltonian with momentum cutoff Λ/b. We must then make the scale transformation appropriate for RG studies of unbinding transitions [6],

$$\mathbf{y}\rightarrow\mathbf{y}'=\mathbf{y}/b, \quad l\rightarrow l'=l/b^{\zeta}, \tag{3.1}$$

where $\zeta=(3-d)/2$ is the roughness exponent. This rescaling ensures that the momentum cutoff of the intermediate Hamiltonian is returned to its original value allowing the process to be repeated iteratively.

The trace over short-wavelength fluctuations described above cannot be performed exactly and so the introduction of a number of approximations is required. Since the scheme presented in this paper is somewhat different from earlier analyses it is appropriate at this stage to discuss the approximations involved and in particular how these differ from the previous studies. One starts, as in the Wilson scheme, by assuming that $l^{>}(\mathbf{y})$ can be expanded thus

$$l^{>}(\mathbf{y})=\sum_n \sqrt{\Omega} l_n^{>} E_n(\mathbf{y}), \tag{3.2}$$

where the $E_n(\mathbf{y})$ are a complete set of suitably chosen eigenfunctions or wave packets which are localized in both real and momentum space. In momentum space this localization simply refers to the restriction of Fourier modes to the shell $\Lambda/b<|\mathbf{k}|<\Lambda$ while in real space the E_n are assumed to be localized in real-space cells of volume $\Omega(b)$. The volume is chosen to be as small as possible while still satisfying the ''uncertainty relation'' [28]

$$\Omega(b)\int_{\Lambda/b}^{\Lambda}\frac{d^{d-1}k}{(2\pi)^{d-1}}=1. \tag{3.3}$$

We then make the following approximations.

(i) First we ignore the overlap between wave packets so that in any real-space cell there is only one nonzero $E_n(\mathbf{y})$. In particular, it is convenient to define [28]

$$\frac{\Omega\Sigma_0}{k_BT}\int\frac{d^{d-1}k}{(2\pi)^{d-1}}\,k^2\tilde{E}_n(\mathbf{k})\tilde{E}_m(-\mathbf{k})=\frac{\delta_{nm}}{\tilde{a}^2}, \tag{3.4}$$

where $\tilde{E}_n(\mathbf{k})$ is the Fourier transform of $E_n(\mathbf{y})$, δ_{nm} is the Kronecker delta, and $\tilde{a}$ is a length scale which at this stage remains arbitrary.

(ii) Secondly, we assume that the large scale fluctuations $l^{<}(\mathbf{y})\equiv l(\mathbf{y})-l^{>}(\mathbf{y})$ may be considered to be constant within each real-space cell, thus we denote the value of $l^{<}(\mathbf{y})$ within cell n by $l_n^{<}$. Note that this step is fundamentally a ''bookkeeping'' procedure in the calculation, important fluctuations in $l^{<}(\mathbf{y})$ should be accounted for by later applications of the iterative procedure. Hence we are not, for example, inferring that $[\nabla l^{<}(\mathbf{y})]$ is zero within each cell with singular behavior at the boundary between cells. In fact we supplement the above assumption with the analogous approximation that $[\nabla l^{<}(\mathbf{y})]$ is also constant within each real-space cell. This addition is essential in order to incorporate the position-dependent stiffness coefficient and is in the spirit of the original scheme.

(iii) Finally it is necessary to make some simplifying assumptions about the eigenfunctions. We retain the traditional approximation that the magnitude of $E_n(\mathbf{y})$ is constant within each real-space cell. The $E_n(\mathbf{y})$ are orthogonal to $l^{<}(\mathbf{y})$ since they have no cross support in momentum space—this leads to the result that if E_n is nonzero in a given cell then $|E_n(\mathbf{y})|\approx\Omega^{-1/2}$ with E_n being positive in one half of the cell and negative in the other half [27]. In addition we ignore variations in $|\nabla E_n(\mathbf{y})|$ which is again required to extend the NFRG to study Eq. (2.9). Note that the value of $|\nabla E_n(\mathbf{y})|$ is fixed by Eq. (3.4) which for $n=m$ can be written

$$\int d^{d-1}y|\nabla E_n(\mathbf{y})|^2=k_BT/\Omega\Sigma_0\tilde{a}^2. \tag{3.5}$$

Hence if we write $\overline{B}=|\nabla E_n|$ then $\overline{B}$ is simply related to the arbitrary length scale $\tilde{a}$ introduced earlier via $\Omega\overline{B}^2=k_BT/\Omega\Sigma_0\tilde{a}^2$.

The approximations we have introduced are seen to be simple extensions of the earlier schemes and do not introduce any new arbitrary length scales into the analysis. Furthermore, these approximations are not in conflict with the analyses of LF and DL; hence if the modified scheme is applied to the traditional capillary-wave model (2.1),

results identical to those of the earlier authors are obtained. Indeed because the extra approximations do not affect the calculation if $\Delta\Sigma(l)\equiv 0$ those original results must also be recovered from the calculations described below in the limit of $\Delta\Sigma(l)\to 0 \forall l$.

B. Recursion relations and flow equations

With the division of the fluctuating field into long-wavelength and short-wavelength parts, $l=l^<+l^>$ described above, the effective Hamiltonian (2.9) can conveniently be written

$$H[l^<+l^>]=H_0[l^<]+H_0[l^>]+H_I[l^<+l^>], \quad (3.6)$$

where

$$H_0[l]=\int d^{d-1}y\,\tfrac{1}{2}\Sigma_0(\boldsymbol{\nabla} l)^2, \quad (3.7)$$

and

$$H_I[l]=\int d^{d-1}y\{\tfrac{1}{2}\Delta\Sigma(l)(\boldsymbol{\nabla} l)^2+V(l)\}. \quad (3.8)$$

With this notation we define the intermediate, unrescaled, renormalized Hamiltonian $H'[l^<]$ say, via the partial trace over short-wavelength fluctuations

$$\exp\{-\beta H'[l^<]\}=\frac{1}{N_0}\exp\{-\beta H_0[l^<]\}\int \mathcal{D}l^> \times\exp\{-\beta(H_0[l^>]+H_I[l^<+l^>])\}, \quad (3.9)$$

where $\beta=1/k_BT$ and the normalization factor $N_0\equiv\int\mathcal{D}l^>\exp\{-\beta H_0[l^>]\}$.

Using the expansion (3.2) we can convert the functional integral into a multidimensional integral over the components $l_n^>$, $\int\mathcal{D}l^>\cdots=\int\Pi_n dl_n^>\cdots$, where we have ignored constant factors which vanish when a ratio is taken. Furthermore, using the approximations discussed above we obtain the simplifications

$$\beta H_0[l^>]=\frac{1}{2}\sum_n\left(\frac{l_n^>}{\tilde{a}}\right)^2 \quad (3.10)$$

and

$$\beta H_I[l^<+l^>]=\sum_n\left\{\frac{1}{2\tilde{\nu}}g(l_n^<,l_n^>)+\left[\frac{(\boldsymbol{\nabla} l_n^<)^2}{4\tilde{\nu}}+\frac{l_n^{>2}}{4\tilde{a}^2\Sigma_0}\right]h(l_n^<,l_n^>)\right\}. \quad (3.11)$$

Here the scale $\tilde{\nu}\equiv\tilde{\nu}(b)=1/\beta\Omega(b)$ and the functions g and h are given by

$$g(x,y)=V(x+y)+V(x-y), \quad (3.12)$$

$$h(x,y)=\Delta\Sigma(x+y)+\Delta\Sigma(x-y). \quad (3.13)$$

Substituting these results into Eq. (3.9) and performing the appropriate integrations yields $H'[l^<]$. To complete the renormalization group step we then rescale according to Eq. (3.1). In this way we find that the initial potential $V^{(0)}(l)\equiv V(l)$ and stiffness contribution $\Delta\Sigma^{(0)}(l)\equiv\Delta\Sigma(l)$ are renormalized via successive applications of $V^{(N+1)}(l)=\mathcal{R}_V[V^{(N)}(l),\Delta\Sigma^{(N)}(l)]$ and $\Delta\Sigma^{(N)+1}(l)=\mathcal{R}_{\Delta\Sigma}[V^{(N)}(l),\Delta\Sigma^{(N)}(l)]$ where [21]

$$\mathcal{R}_V\equiv-\tilde{\nu}b^{d-1}\ln\left[\int_{-\infty}^{\infty}\frac{dl'}{(2\pi)^{1/2}\tilde{a}}E(l,l')\right] \quad (3.14)$$

and

$$\mathcal{R}_{\Delta\Sigma}\equiv\frac{\int_{-\infty}^{\infty}dl'h(b^\zeta l,l')E(l,l')}{2\int_{-\infty}^{\infty}dl''E(l,l'')}, \quad (3.15)$$

where for brevity we have introduced the function E given by

$$E(x,y)=\exp\left\{-\frac{y^2}{2\tilde{a}^2}-\frac{1}{2\tilde{\nu}}g(b^\zeta x,y)-\frac{y^2}{4\Sigma_0\tilde{a}^2}h(b^\zeta x,y)\right\}. \quad (3.16)$$

The RG described above displays many similarities with the earlier analysis of LF as should be expected since the earlier results must be recovered when $\Delta\Sigma\equiv 0$. We therefore anticipate, as verified below, that the ''arbitrary'' length scale $\tilde{a}$ should be fixed to the same value derived by LF,

$$\tilde{a}^2(b)=\frac{k_BT}{\Sigma_0}\int_{\Lambda/b}^{\Lambda}\frac{d^{d-1}k}{(2\pi)^{d-1}k^2}. \quad (3.17)$$

However, the inclusion of the $\Delta\Sigma(l)$ term leads to fundamental changes in the final results, with most notably the RG flow of the binding potential being intrinsically linked to that of $\Delta\Sigma$ as embodied in Eq. (3.14). Further, Eq. (3.15) reveals a subtle interplay between the flows of the two functions with the explicit dependence of $\Delta\Sigma^{(N+1)}(l)$ on $V^{(N)}(l)$.

In the infinitesimal rescaling limit $b=e^{\delta t}$ ($\delta t\to 0$) with $\tilde{a}^2$ given by Eq. (3.17) the recursion relations (3.14) and (3.15) yield coupled flow equations

$$\frac{\partial V}{\partial t}=(d-1)V+\zeta l\frac{\partial V}{\partial l}+\Sigma_0\Lambda^2\omega\xi_b^2\ln\left[1+\frac{1}{\Sigma_0\Lambda^2}\times\left\{\frac{\partial^2 V}{\partial l^2}+\Lambda^2\Delta\Sigma\right\}\right], \quad (3.18)$$

and

$$\frac{\partial\Delta\Sigma}{\partial t}=\zeta l\frac{\partial\Delta\Sigma}{\partial l}+\omega\xi_b^2\frac{\partial^2\Delta\Sigma}{\partial l^2}\left[1+\frac{1}{\Sigma_0\Lambda^2}\times\left\{\frac{\partial^2 V}{\partial l^2}+\Lambda^2\Delta\Sigma\right\}\right]^{-1}, \quad (3.19)$$

where $\omega\equiv\omega(d)$ is the generalization to arbitrary dimension of the wetting parameter introduced in Eq. (2.3),

$$\omega(d)=\frac{k_BT}{4\pi\Sigma_0\xi_b^2\Gamma[(d-1)/2]}\left(\frac{\Lambda^2}{4\pi}\right)^{(d-3)/2}. \quad (3.20)$$

C. Linear limit

In this subsection we briefly confirm that the nonlinear scheme described above is exact to leading order in both the binding potential and position-dependent stiffness contribution. First we note that the linearized recursion relation for $\Delta\Sigma(l)$ which follows from Eq. (3.15) is

$$\Delta\Sigma^{(N+1)}(l)=\int_{-\infty}^{\infty}\frac{dl'}{(2\pi)^{1/2}\tilde{a}}\,e^{-l'^2/2\tilde{a}^2}\Delta\Sigma^{(N)}(b^\zeta l-l'). \quad (3.21)$$

This agrees precisely with the linearized recursion relation derived by FJ provided we make the identification (3.17) for $\tilde{a}^2$. The resulting flow equation, which is exact at this order, is

$$\frac{\partial\Delta\Sigma}{\partial t}=\zeta l\,\frac{\partial\Delta\Sigma}{\partial l}+\omega\xi_b^2\,\frac{\partial^2\Delta\Sigma}{\partial l^2}, \quad (3.22)$$

which also follows directly from linearizing Eq. (3.19). When working at this order the flow of $\Delta\Sigma(l)$ is independent of the binding potential; as we have seen above this is not the case at higher orders.

For $V(l)$ the linearized recursion relation arising from Eq. (3.14) is

$$V^{(N+1)}(l)=b^{d-1}\int_{-\infty}^{\infty}\frac{dl'}{(2\pi)^{1/2}\tilde{a}}\,e^{-l'^2/2\tilde{a}^2}\left\{V^{(N)}(b^\zeta l-l')+\frac{\omega\xi_b^2\Lambda^2}{(d-1)}[1-b^{1-d}](l'/\tilde{a})^2\Delta\Sigma^{(N)}(b^\zeta l-l')\right\}, \quad (3.23)$$

where we have made use of the relation $\tilde{\nu}/2\Sigma_0\equiv[1-b^{1-d}]\omega\xi_b^2\Lambda^2/(d-1)$. The expression in curly brackets differs slightly from that found by FJ where the factor $(l'/\tilde{a})^2$ is absent [cf. Eq. (2.11) where $d=3$ and $b=e^t$]. Importantly this difference is of no consequence in the derivation of the flow equation where we set $b=e^{\delta t}$ and look for terms of $O(\delta t)$ on the right-hand side of Eq. (3.23). Noting $[1-b^{1-d}]/(d-1)=O(\delta t)$ and $\int dl'\,e^{-l'^2/2\tilde{a}^2}[(l'/\tilde{a})^2-1]\Delta\Sigma(b^\zeta l-l')/(2\pi)^{1/2}\tilde{a}=O(\delta t)$ confirms that the expressions are equivalent in the infinitesimal rescaling limit. Thus using Eq. (3.23) we derive the exact result

$$\frac{\partial V}{\partial t}=(d-1)V+\zeta l\,\frac{\partial V}{\partial l}+\omega\xi_b^2\left\{\frac{\partial^2 V}{\partial l^2}+\Lambda^2\Delta\Sigma\right\}, \quad (3.24)$$

for the linearized flow equation, consistent both with FJ and Eq. (3.18).

D. Hard-wall restrictions

In addition to including nonlinear terms, a key feature of the NFRG compared with linear RG studies is the ability to incorporate a true hard wall $V(l)=\infty$ for $l<0$ (see Sec. II B). This ensures that the fluctuating field $l(\mathbf{y})$ always remains in front of the wall as is physically desirable. Here we derive the appropriate recursion relations when a hard wall is present and examine its relevance for $\Delta\Sigma(l)$. First we note from Eq. (3.14) that if we include a hard wall in our initial bare potential it remains fixed at $l=0$ under iterations of $\mathcal{R}_V$. Thus

$$V^{(N)}(l)=\infty \quad \text{for } l<0, \quad (3.25)$$

for all N if $V^{(0)}(l<0)=\infty$. Furthermore, for $l>0$ we observe

$$V^{(N+1)}(l)=-\tilde{\nu}b^{d-1}\ln\left[\left(\frac{2}{\pi}\right)^{1/2}\int_0^{b^\zeta l}\frac{dl'}{\tilde{a}}\,E^{(N)}(l,l')\right], \quad (3.26)$$

where we have used the symmetry $E(l,-l')=E(l,l')$ in order to restrict the integral to $l'>0$. In Eq. (3.26) $E^{(N)}$ refers to the function E with potential $V\equiv V^{(N)}(l)$ and stiffness $\Delta\Sigma\equiv\Delta\Sigma^{(N)}(l)$.

Similarly in the presence of a hard wall the stiffness contribution recursion relation (3.15) reduces to

$$\Delta\Sigma^{(N+1)}(l)=\frac{\int_0^{b^\zeta l}dl'\,h^{(N)}(b^\zeta l,l')E^{(N)}(l,l')}{2\int_0^{b^\zeta l}dl''E^{(N)}(l,l'')}, \quad (3.27)$$

for $l>0$ where $h^{(N)}$ can be read from Eq. (3.13) replacing $\Delta\Sigma$ by $\Delta\Sigma^{(N)}$. It follows from these last two relations that in calculating $V^{(N+1)}(l)$ and $\Delta\Sigma^{(N+1)}(l)$ for $l>0$ we need never specify $\Delta\Sigma^{(N)}(l)$ with $l<0$. Thus if we assume a hard-wall initial potential $V^{(0)}(l<0)=\infty$ then the form of $\Delta\Sigma^{(0)}(l<0)$ is completely irrelevant and can most simply be assumed zero.

IV. NUMERICAL STUDY

In this section we provide a detailed numerical study based on the nonlinear recursion relations derived above. We shall show that both critical and first-order transitions are found and give realistic estimates for the location of the tricritical point separating the two behaviors. The bulk of the calculations described here have been performed with fixed rescaling factor $b=2$. However, we conclude by considering, in a numerical manner, the effect on these results of approaching the infinitesimal rescaling limit $b\to1^+$.

A. Fixed points

The critical phenomena of our model will be governed by the fixed points $(V^*(l),\Delta\Sigma^*(l))$ of Eqs. (3.14) and (3.15). It is convenient to rewrite the flow equations (3.18) and (3.19) using the dimensionless variables

$$z\equiv l\sqrt{2\zeta}/A,$$

$$U(z)\equiv 2\zeta V(Az/\sqrt{2\zeta})/B, \quad (4.1)$$

$$S(z)=A^2\Lambda^2\Delta\Sigma(Az/\sqrt{2\zeta})/B,$$

where A and B are b-independent parameters defined by

$$A \equiv \left[\frac{\tilde{a}^2(b)(3-d)}{b^{3-d}-1} \right]^{1/2} = \xi_b \sqrt{2\omega(d)} \tag{4.2}$$

and

$$B \equiv \frac{\tilde{\nu}(b)(d-1)}{1-b^{1-d}} = \frac{2\Lambda^{d-1} k_B T}{(4\pi)^{(d-1)/2}\Gamma[(d-1)/2]}. \tag{4.3}$$

In this case the flow equations simplify to

$$\frac{\partial U}{\partial t} = \zeta \left(\tau U + z \frac{\partial U}{\partial z} + \ln\left[1 + \frac{\partial^2 U}{\partial z^2} + S \right] \right) \tag{4.4}$$

and

$$\frac{\partial S}{\partial t} = \zeta \left(z \frac{\partial S}{\partial z} + \frac{\partial^2 S}{\partial z^2} \left[1 + \frac{\partial^2 U}{\partial z^2} + S \right]^{-1} \right), \tag{4.5}$$

where τ is as given in Eq. (2.5) and recall $\zeta = (3-d)/2$.

With this notation we are interested in fixed-point pairs $(U^*(z), S^*(z))$ which satisfy $\partial U^*/\partial t = \partial S^*/\partial t = 0$ along with the boundary conditions of a hard wall $[U^*(z<0) = \infty]$ and U^* and S^* decaying to zero for large z. The appropriately rescaled fixed-point potentials of DL, discussed in Sec. II B, in combination with the trivial stiffness contribution $S(z) \equiv 0$ are clearly fixed points of the system. In general, extending the procedure described by Lipowsky [29] we search for fixed points starting at small z with the local conditions $U^*(z) \approx \sigma_1 / z^\tau$, $S^*(z) \approx \sigma_2$, where the σ_i are constants, and integrate forward. The tails of $U^*(z)$ and $S^*(z)$ arising for large z can be determined by linearizing Eqs. (4.4) and (4.5). Thus we find

$$S^*(z) = \rho_s \int_z^\infty dz' \ \exp(-z'^2/2) \tag{4.6}$$

and

$$U^*(z) = \rho_1 He_{\tau-1}(z) + \frac{\rho_2}{z^\tau} \left(1 + \sum_{N=1}^{\infty} \frac{(\tau+2N-1)!}{N!(\tau-1)!} \frac{1}{2z^{2N}} \right) - \frac{1}{\tau} S^*(z) \tag{4.7}$$

for large z, where $\mathrm{He}_{\tau-1}(z)$ is the Hermite polynomial of order $\tau-1$ and ρ_s, ρ_1, ρ_2 are arbitrary constants. For fixed-point potentials in the strong-fluctuation regime we must choose initial parameters which yield $\rho_2 = 0$. A preliminary study employing this procedure suggests that a family of fixed-point pairs exist, parametrized by σ_2. However, we find that the magnitude of $S^*(z)$ is only non-negligible in the region where $U^*(z)$ is so large that it is effectively infinite, i.e., for $z \to 0$. Thus typically one finds a fixed-point potential picture indistinguishable from that of DL.

B. Dimensionless variables

For the calculations described below it is convenient to follow the lead of LF and absorb the scale factors $\tilde{a}(b)$ and $\tilde{\nu}(b)$ into our functions. Thus, using a notation similar to that above but now for fixed $b > 1$, we define

$$z \equiv l/\sqrt{2}\tilde{a}(b),$$
$$U^{(N)}(z) \equiv V^{(N)}[\sqrt{2}\tilde{a}(b)z]/\tilde{\nu}(b), \tag{4.8}$$
$$S^{(N)}(z) \equiv \Delta\Sigma^{(N)}[\sqrt{2}\tilde{a}(b)z]/\Sigma_0.$$

In this way z, U, and S are dimensionless variables and the rescaled recursion relations have no explicit dependence on the cutoff Λ. In particular, we obtain

$$U^{(N+1)}(z) = -b^{d-1} \ln\left[\frac{2}{\sqrt{\pi}} \int_0^\infty dz' \mathcal{E}(z,z') \right] \tag{4.9}$$

for the rescaled binding potential, and

$$S^{(N+1)}(z) = \frac{\int_0^\infty dz' [S^{(N)}(b^\zeta z + z') + S^{(N)}(b^\zeta z - z')] \mathcal{E}(z,z')}{2\int_0^\infty dz'' \mathcal{E}(z,z'')} \tag{4.10}$$

for the stiffness contribution. Here $\mathcal{E}$ is given by

$$\mathcal{E}(z,z') = e^{-z'^2 - [U^{(N)}(b^\zeta z + z') + U^{(N)}(b^\zeta z - z')]/2} \times e^{-z'^2 [S^{(N)}(b^\zeta z + z') + S^{(N)}(b^\zeta z - z')]/2}. \tag{4.11}$$

In both recursion relations (4.9) and (4.10) we can replace the upper limit of the integrals by $b^\zeta z$ upon assuming a hard-wall potential.

C. Phase diagram

For systems with purely short-ranged forces it suffices to consider a bare potential [6]

$$U^{(0)}(z) = \begin{cases} -we^{-sz} + e^{-2sz}, & z > 0 \\ \infty, & z < 0 \end{cases} \tag{4.12}$$

where w is a measure of the deviation from the mean-field wetting temperature $w \propto T_W^{\mathrm{MF}} - T$, and $s > 0$. For $z > 0$ additional terms with coefficients which vanish at the MF wetting temperature may be included and the coefficient of the e^{-2sz} term need not be set to unity but can be included as an additional parameter in the model. These modifications will alter the precise location of phase boundaries but do not affect the critical phenomena discussed below. For the bare position-dependent stiffness contribution we write [13]

$$S^{(0)}(z) = \begin{cases} -qsze^{-2sz}, & z > 0 \\ 0, & z < 0 \end{cases} \tag{4.13}$$

where the parameter q is the *stiffness strength*. Recall that the form of $S^{(0)}(z<0)$ is arbitrary, given the hard-wall contribution to the potential. Again, for $z > 0$ further terms such as e^{-sz} with a coefficient which vanishes at $T = T_W^{\mathrm{MF}}$ may be included [12] but these do not affect the essential physics. The advantage of modeling $U^{(0)}$ and $S^{(0)}$ by Eqs. (4.12) and (4.13) is that the results of LF are recovered exactly in the limit $q \to 0$.

To determine the phase boundary we numerically iterate the potential and stiffness contribution using the recursion relations (4.9) and (4.10) with fixed $b = 2$, starting with the bare functions (4.12) and (4.13). In this way we find a two-

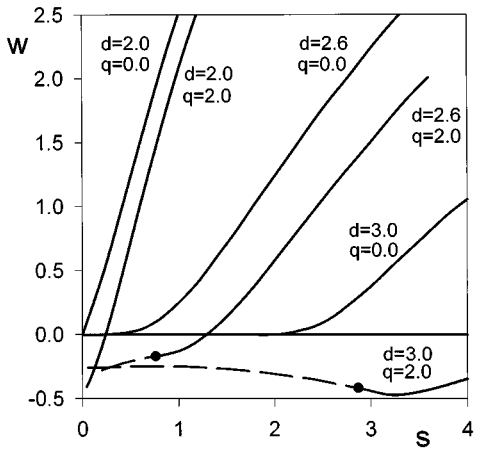

FIG. 2. Phase boundaries in the (w,s) plane for the dimensionally reduced bare potential and position-dependent stiffness contributions given by Eqs. (4.12) and (4.13), respectively, calculated with $b=2$. Recall w measures the deviation from the mean-field wetting temperature $w \propto T_W^{\mathrm{MF}} - T$. The various phase boundaries are labeled by dimension d and stiffness strength q. The region above a boundary line corresponds to the ''bound'' phase while that below represents the unbound or delocalized interface. Solid lines denote critical loci while dashed lines correspond to first-order loci; tricritical points separating the two regimes are shown by thick dots.

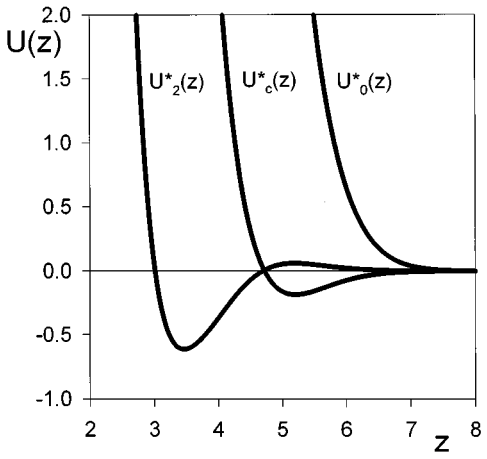

FIG. 3. The three fixed-point potentials $U_0^*(z)$, $U_c^*(z)$, and $U_2^*(z)$ for dimension $d=2.6$ and rescaling factor $b=2$ [using the dimensionless variables (4.8)]. The corresponding stiffness contributions $S^*(z)$ which make up the fixed-point pairs are all zero (within the precision of our numerical calculations) in the region shown.

dimensional separatrix which divides the three-dimensional parameter space (w,s,q) into ''bound'' and ''unbound'' regions. The intersections of this separatrix with planes of fixed q are shown in Fig. 2 for both $q=0$ (corresponding to LF) and $q=2$ for a range of dimensions. Unlike the earlier study one finds that three fixed-point potentials are important in mapping out phase space. In addition to $U_c^*(z)$ and $U_0^*(z)$ [using the rescaling (4.8)] the attractive manifold of the potential $U_2^*(z)$ [corresponding to $V_2^*(l)$ of DL] is also relevant. For fixed d let $w_c(s,q)$ represent the separatrix. For $w<w_c$ the attractive part of $U^{(N)}$ decays to zero eventually being mapped to $U_0^*(z)$ which governs the completely unbound phase. For $w>w_c$ the minimum of $U^{(N)}$ becomes deeper and deeper, representing the bound phase in which the interfacial separation remains finite. For $w=w_c$ the potential is governed by one of the multicritical fixed points $U_c^*(z)$ or $U_2^*(z)$. For $d=2.6$ these three fixed-point potentials are shown in Fig. 3. Crossing the phase boundary from the U_c^* to U_0^* region corresponds to critical wetting since the minimum of $U(z)$ diverges continuously to infinity as $U(z)$ transforms continuously from U_c^* to U_0^* (as assumed happens when crossing between different RG fixed-point regions). Similarly the transition between the U_2^* and U_0^* regions is first-order wetting since the minimum of $U(z)$ jumps discontinuously from a finite value to infinity as $U(z)$ transforms continuously from U_2^* to U_0^*. The potential U_0^* is easily found numerically since it is completely stable [6]. Hence if we start in any region of phase space satisfying $w<w_c$ we eventually iterate to the fixed point. The second fixed point U_c^* is a little more difficult to reach because it has one relevant (unstable) perturbation so we must choose starting parameters within that region of the plane $w=w_c$ corresponding to critical wetting. The final fixed point is particularly difficult to determine because U_2^* has two relevant perturbations. Thus only with starting parameters in the plane $w=w_c$ *on the line dividing critical and first-order transitions* do we eventually flow to the fixed point. The general topology of phase space for binding potentials in the strong-fluctuation regime is shown schematically in Fig. 4.

Returning to the phase diagram we note that for fixed $q<0$ no first-order transitions are found since the stiffness contribution strengthens rather than destabilizes the critical wetting transition. Similarly, recall for $d \lesssim 2.41$ that the fixed point U_2^* is not present so once again only critical wetting can occur. Hence in $d=2$ it is the scaling index of the only relevant perturbation at $U_c^*(z)$ which is important for determining the critical exponents, thus as with LF one finds $\nu_{\|} = (0.49 \pm 0.01)^{-1}$ in excellent agreement with the exact value $\nu_{\|}=2$ [22]. For larger $d \gtrsim 2.41$ first-order phase bound-

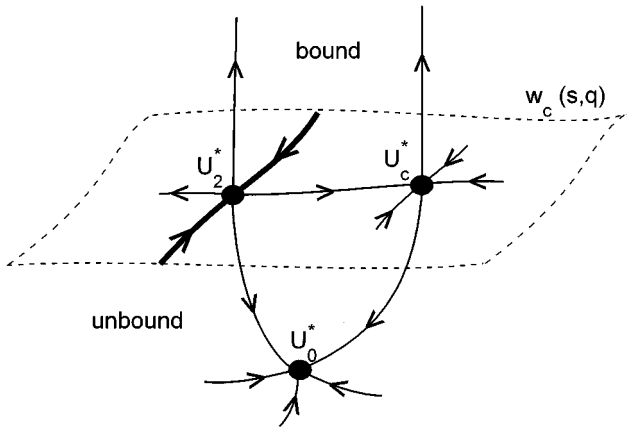

FIG. 4. Schematic representation of the topology of phase space when the three fixed-point potentials U_0^*, U_c^*, and U_2^* are all relevant. The separatrix w_c divides the regions of phase space corresponding to bound and unbound interfaces while the thick line is a line of tricritical points separating first-order and critical wetting.

aries are possible and occur (for fixed $q>0$) for small values of s. For large s the transition remains critical; a tricritical point s_t separates these two regions. It is found, as also seen in Fig. 2, that at fixed d the region of the phase diagram in which the interface remains bound increases with q. We also note that for $d=3$, $q=2.0$ the value of s at the tricritical point $s_t \approx 2.83$ (corresponding to $\omega_t \approx 2.89$) is much higher than earlier estimates by FJ.

D. The stiffness instability in $d=3$

Recall that the FJ stiffness instability mechanism proposes that in $d=3$ the bare critical wetting transition could be driven fluctuation-induced first order (see Sec. II C). We have seen above how this mechanism may arise in general and in this subsection we provide a semiquantitative analysis to locate more accurately the tricritical point ω_t in three dimensions for relevant temperatures. To this end we must provide an estimate for the stiffness strength q in $d=3$. This is achieved by first noting from the analysis of FJ that, neglecting terms of $O(T_W^{\mathrm{MF}}-T)$, $V(l)\sim v_{20}e^{-2\kappa l}+\cdots$ and $\Delta\Sigma(l)\sim s_{21}\kappa l e^{-2\kappa l}+\cdots$. Furthermore, we observe that the simple relation

$$s_{21}\approx -2v_{20} \tag{4.14}$$

appears to be generally true at mean-field level. We shall not go into detail here but just note that this relation holds exactly for the integral and simple crossing constraint choices for the collective coordinate l [12,13], and for a more generalized crossing constraint definition of l [30]. From the rescaling (4.8) the bare potential $U^{(0)}(z)$ corresponds to the choice $v_{20}=\tilde{\nu}(b)$ and hence using Eq. (4.13) one should choose $q\approx 2\tilde{\nu}(b)/\Sigma_0$. Substituting for $\tilde{\nu}(b)$ and recalling $d=3$ yields

$$q\approx k_B T\Lambda^2(1-1/b^2)/2\pi\Sigma_0. \tag{4.15}$$

Consequently, for rescaling factor $b=2$ we have $q\approx 3\omega(T)\xi_b^2\Lambda^2/2$ [31], where $\omega(T)$ is the wetting parameter defined earlier.

For the simple-cubic Ising model (appropriate to simulations) $\omega(T)$ has been estimated by Fisher and Wen [24] to be in the range $0.70<\omega(T)<0.87$ for $0.55<T/T_c<1.0$ while the wetting temperature lies in the range $0.6<T_W/T_c<0.93$. It is reasonable to assume a lattice cutoff $\Lambda\approx\pi/a$ where a is the simple-cubic lattice spacing. Using this in combination with estimates by Evans, Hoyle, and Parry [32] for the true bulk correlation length yields $\Lambda^2\xi_b^2\approx 1.3$ at $T=0.6T_c$ increasing monotonically to $\Lambda^2\xi_b^2\approx 10.0$ at $T=0.93T_c$. Thus sensible estimates of q lie in the range $1.41<q<12.0$. In particular, we find that the appropriate estimate for q increases with temperature so that, for example, we predict $q(T=0.6T_c)\approx 1.41$, $q(T=0.7T_c)\approx 2.46$, $q(T=0.8T_c)\approx 4.41$, and $q(T=0.9T_c)\approx 9.96$ for the choice $b=2$. If we take $q=0.9$, considerably lower than the above estimates, we already find that the tricritical point $\omega_t(=s_t^2/4\ln b)\approx 2.07$, again significantly larger than earlier predictions. Similarly for $q=1.41$ we find $\omega_t\approx 2.49$ while as mentioned above for $q=2.0$, $\omega_t\approx 2.89$. As the value of q increases the tricritical point location also moves to higher values. Clearly these quoted values of ω_t will depend to some extent on the approximations used above, for example, on the choice of cutoff Λ. Furthermore, we have not at this stage considered how significant a role the choice of fixed $b=2$ plays (see below). However, given that ω_t is around three times the value of current estimates for $\omega(T)$, we can predict at this stage that the mean-field critical wetting transition is actually fluctuation-induced first order.

E. The rescaling parameter b and the infinitesimal rescaling limit

Now we focus on how relevant the choice of rescaling factor b is for our quantitative results and provide some general results for how the location of the tricritical point varies with b, d, and q. Recall that the NFRG is an approximate technique being exact only to first order in the binding potential and position-dependent stiffness contribution. Thus the NFRG scheme does not possess the semigroup property which would ensure the results would be insensitive to the choice of b. Hence ideally we would like to consider the infinitesimal rescaling limit $b=1^+$, however, this is not possible using the numerical scheme described above. To overcome this problem we have studied a range of rescaling parameters $1.125\leqslant b\leqslant 5$ numerically and extrapolate our results to the infinitesimal limit.

We focus here on the location of the tricritical point s_t in this limit. Our first observation from this analysis is that the s_t vanish as $b\to 1$ in a logarithmic manner. In particular, we find $s_t\propto\sqrt{\ln b}$. This behavior is not surprising and is in fact essential if the general scenario presented above is not to be fundamentally changed. This is the case because the physically interesting quantity is not s_t but ω_t which is related to s_t by

$$\omega_t=\frac{s_t^2}{4\ln b[1+O(\epsilon\ln b)]}, \tag{4.16}$$

where $\epsilon=3-d$. Thus if s_t decayed to zero any faster than $O(\sqrt{\ln b})$ as $b\to 1$ then the tricritical point $\omega_t\to 0$ in the infinitesimal limit and so the fluctuation-induced first-order wetting would be effectively lost. Likewise, if s_t decays to zero more slowly than $O(\sqrt{\ln b})$ (or $s_t\not\to 0$ as $b\to 1$) then in the infinitesimal limit $\omega_t\to\infty$ and the bare critical wetting transition would always be driven first order. Hence only with the observed $\sqrt{\ln b}$ vanishing can ω_t remain at a finite nonzero value.

The remaining b dependence of the s_t is found to be in excellent agreement with a simple linear fit in $1/b$. This is shown in Fig. 5 when $q=0.9$ for the range of dimensions $2.60<d<2.84$. Results at higher dimensions are fully consistent with this simple fit although fewer data have been gathered due to increased calculation times. In general we find that the location of the tricritical point can be written as

$$s_t\approx\mathcal{S}(q,\epsilon)\sqrt{\ln b}\left(1-\frac{B}{b}\right), \tag{4.17}$$

where $B=0.49$ and $\mathcal{S}(q,\epsilon)$ is a b-independent function which we determine below. This reveals a quite significant

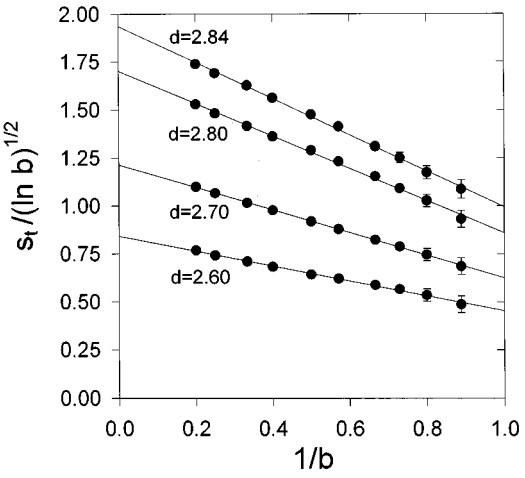

FIG. 5. Location of the tricritical point s_t (rescaled by $\sqrt{\ln b}$) plotted as a function of $1/b$ for $q=0.9$ and a range of dimensions. A linear fit to each data set is given. Where error bars are not shown the error lies within the size of the symbol. Note that upon extrapolating we find that all the lines have a common point of intersection on the $s_t=0$ axis at the location $1/b\approx 2.04$.

effect upon ω_t in taking the infinitesimal limit since extrapolating and using Eq. (4.16) yields

$$\omega_t(b=1^+)\approx 0.46\omega_t(b=2). \tag{4.18}$$

Hence the results above for ω_t calculated using $b=2$ are predicted to be reduced to a little under half their given values, in the infinitesimal limit. Nevertheless the resulting tricritical values are still comfortably larger than the corresponding predictions for $\omega(T)$ so that our conclusions remain unaltered. However, this large change in going from $b=2$ to $b=1$ does demonstrate how careful we must be in extracting quantitative results using the NFRG.

We conclude by providing some details of the function $\mathcal{S}(q,\epsilon)$ introduced in Eq. (4.17). From our numerical studies we find that this function can most easily be written in the form

$$\mathcal{S}(q,\epsilon)=q^{f_1(\epsilon)}f_2(\epsilon), \tag{4.19}$$

where $f_1(\epsilon)$ and $f_2(\epsilon)$ are dimension-dependent functions with f_1 given by

$$f_1(\epsilon)\approx 0.206+0.50\epsilon, \tag{4.20}$$

while f_2 can be written as a simple expansion in ϵ,

$$f_2(\epsilon)\approx\sum_{n=0}^{4} f_2^{(n)}\epsilon^n, \tag{4.21}$$

with $f_2^{(0)}=3.90$, $f_2^{(1)}=-18.69$, $f_2^{(2)}=57.68$, $f_2^{(3)}=98.08$, and $f_2^{(4)}=59.42$. This expansion is valid for those dimensions for which a tricritical point exists, i.e., $\epsilon\lesssim 0.59$. The weak dependence of s_t on q implied by Eq. (4.20) reveals that our results are robust to uncertainties in our choice of stiffness strength. Recall that our approximations for the cutoff Λ and wetting parameter ω are contained within the estimate for q. Thus our quoted values of q, although reasonable, are clearly only approximate. However, using Eq. (4.20) close to $d=3$ ($\epsilon=0$) reveals that even if we let q vary by $\pm 50\%$, say, then the resulting tricritical point location s_t varies by less than $\pm 14\%$. Hence even in the worst possible scenario for both b and q we confidently predict $\omega_t>\omega(T)$ and thus expect a first-order wetting transition.

V. DISCUSSION AND CONCLUSIONS

We have studied the effect of a position-dependent stiffness contribution $\Delta\Sigma(l)$ on the critical behavior related to an unbinding or wetting transition. In particular, we have introduced a modified functional renormalization group scheme which allows a nonlinear analysis of effective Hamiltonian models containing nonzero $\Delta\Sigma(l)$. The resulting flow equations, which are exact at linear order in $\Delta\Sigma(l)$ and the binding potential $V(l)$, reveal a delicate coupling between the flows of V and $\Delta\Sigma$.

In the strong-fluctuation regime the unbinding transition is governed by three nontrivial fixed points leading to the possibility of both critical and first-order transitions. Specifically, first-order transitions become possible for spatial dimensions $d\gtrsim 2.41$. This differs significantly from the case of a position-independent stiffness coefficient when only critical transitions are found for all d.

In contrast to the earlier linear RG analysis, our approach allows results on the location and order of the wetting transition to be determined with semiquantitative accuracy (these have typically been computed with rescaling factor $b=2$). We have further considered the approach to the infinitesimal rescaling limit in a numerical fashion in order to quantitatively understand the effect of this parameter on our results. In each case, for temperatures $0.6<T_W/T_c<0.93$ appropriate for comparison with simulations, we confidently predict that in $d=3$ the bare critical wetting transition is fluctuation-induced first order. These results are shown to be robust under large variations in the stiffness strength.

Recall that the linear RG analysis of Jin and Fisher [13] predicted that the first-order transition in $d=3$ would be very weak and thus may be extremely difficult to observe in simulations. We have not addressed the issue of the strength of the transition in this paper but this topic should be considered in future work. However, we note that because of the drifting nature of the fixed points in the approach to $d=3$ it seems likely that in this limit the first-order transition will occur only for very large values of the interface separation l (with l increasing continuously up to that point). Thus we also anticipate a weakly first-order transition. A more analytical approach would be welcome but since this should be based on the coupled nonlinear flow equations significant progress may prove difficult.

ACKNOWLEDGMENTS

I am indebted to Joseph O. Indekeu for many helpful discussions during the course of this work. In addition, the interest, comments, and assistance of Enrico Carlon, Francis Clarysse, Michael E. Fisher, Andrew O. Parry, and Attilio L. Stella have been greatly appreciated. This work was supported by the K. U. Leuven Research Fund (Grant No. F/96/74), the EC Training and Mobility of Researchers programme (Contract No. ERB-FMBI-CT96-1840), the Inter-University Attraction Poles (IUAP), and the Concerted Action Research Programme (GOA).

[1] For a general review of wetting, see S. Dietrich, in *Phase Transitions and Critical Phenomena*, edited by C. Domb and J. L. Lebowitz (Academic, London, 1988), Vol. 12, p. 1.
[2] H. Nakanishi and M. E. Fisher, Phys. Rev. Lett. **49**, 1565 (1982).
[3] R. Lipowsky, D. M. Kroll, and R. K. P. Zia, Phys. Rev. B **27**, 4499 (1983); E. Brézin, B. Halperin, and S. Leibler, J. Phys. (France) **44**, 775 (1983).
[4] R. Lipowsky, Phys. Rev. Lett. **52**, 1429 (1984).
[5] D. S. Fisher and D. A. Huse, Phys. Rev. B **32**, 247 (1985).
[6] R. Lipowsky and M. E. Fisher, Phys. Rev. Lett. **57**, 2411 (1986); Phys. Rev. B **36**, 2126 (1987).
[7] K. Binder, D. P. Landau, and D. M. Kroll, Phys. Rev. Lett. **56**, 2272 (1986); K. Binder and D. P. Landau, Phys. Rev. B **37**, 1745 (1988); K. Binder, D. P. Landau, and S. Wansleben, *ibid.* **40**, 6971 (1989).
[8] T. Halpin-Healy and E. Brézin, Phys. Rev. Lett. **58**, 1220 (1987).
[9] G. Gompper and D. M. Kroll, Europhys. Lett. **5**, 49 (1988).
[10] A. O. Parry and R. Evans, Phys. Rev. Lett. **64**, 439 (1990); Physica A **181**, 250 (1992).
[11] F. David and S. Leibler, Phys. Rev. B **41**, 12 926 (1990). The presence of additional fixed points was also noted in S. Grotehans and R. Lipowsky, Phys. Rev. A **41**, 4574 (1990).
[12] M. E. Fisher and A. J. Jin, Phys. Rev. Lett. **69**, 792 (1992).
[13] A. J. Jin and M. E. Fisher, Phys. Rev. B **47**, 7365 (1993); **48**, 2642 (1993).
[14] K. Binder, D. P. Landau, and A. M. Ferrenberg, Phys. Rev. Lett. **74**, 298 (1995); Phys. Rev. E **51**, 2823 (1995).
[15] C. J. Boulter and A. O. Parry, Phys. Rev. Lett. **74**, 3403 (1995); A. O. Parry and C. J. Boulter, Phys. Rev. E **53**, 6577 (1996).
[16] S. Flesia, Europhys. Lett. **38**, 113 (1997).
[17] For a review of the two-field model of wetting, see A. O. Parry, J. Phys. Condens. Matter **8**, 10 761 (1996).
[18] A. O. Parry and P. S. Swain, Physica A (to be published).
[19] Here the quoted field strengths are measured in units of J, the spin-spin coupling strength in the Ising model.
[20] C. J. Boulter, Phys. Rev. Lett. **79**, 1897 (1997).
[21] The notation we use for describing recursion relations is somewhat ambiguous but is retained for consistency with earlier studies. In practice, for example, the expression $\mathcal{R}[V(l)]$ actually refers to a partial functional $\mathcal{R}[V(l)]=\int dl' f(l,l')$ where f is some function depending implicitly on V.
[22] D. B. Abraham, Phys. Rev. Lett. **44**, 1165 (1980).
[23] M. E. Fisher and A. J. Jin, Phys. Rev. B **44**, 1430 (1991).
[24] M. E. Fisher and H. Wen, Phys. Rev. Lett. **68**, 3654 (1992).
[25] K. G. Wilson, Phys. Rev. B **4**, 3184 (1971); K. G. Wilson and M. E. Fisher, Phys. Rev. Lett. **28**, 240 (1972).
[26] The NFRG approach for tensionless membranes was developed by R. Lipowsky and S. Leibler, Phys. Rev. Lett. **56**, 2541 (1986).
[27] An excellent introduction to Wilson's RG is given in S.-K. Ma, *Modern Theory of Critical Phenomena* (Benjamin, Reading, MA, 1976).
[28] For a review of fluctuation and RG theories applied to interfaces see G. Forgacs, R. Lipowsky, and T. Nieuwenhuizen, in *Phase Transitions and Critical Phenomena*, edited by C. Domb and J. L. Lebowitz (Academic, London, 1991), Vol. 14, p. 135.
[29] R. Lipowsky, Europhys. Lett. **7**, 255 (1988).
[30] C. J. Boulter and J. O. Indekeu, Phys. Rev. E **56**, 5734 (1997).
[31] The stiffness strength estimate embodied in Eq. (4.15) is larger than that given in [20], where a factor of 2 was inadvertently dropped.
[32] R. Evans, D. C. Hoyle, and A. O. Parry, Phys. Rev. A **45**, 3823 (1992).